MICRO LABS LIMITED

SMART DENTAL UPDATES

Dear Doctor,
Greetings from Micro Labs Limited.
This issue contains

- Maxillary Second Molar Tooth with a Single Root and Canal: Endodontic Management
- High-speed cine-magnetic resonance imaging based on T2-weighted sequences for evaluation of velopharyngeal function
- Comparison of intraoral scan and desktop scan of study models

Should you require any specific article or medical information, please feel free to contact us at medicalservices@microlabs.in

Looking forward to your valuable feedback

Best Regards,
Medical Team, Micro Labs Limited

Maxillary Second Molar Tooth with a Single Root and Canal: Endodontic Management

A 32-year-old female reported with a chief complaint of pain in the upper left back tooth, which she reported was increasing while biting and taking cold or hot beverages. The patient's medical history was noncontributory. On clinical examination, there was deep proximal caries with the maxillary left second molar; thus, intraoral periapical radiograph (IOPA) of tooth 27 was advised. The tooth was nonmobile, and periodontal probing was also within the physiological limit. Radiographic examination revealed the carious exposure of tooth 27, and thus, root canal treatment of the teeth was advised. Radiographic examination also revealed some variation in root canal anatomy with tooth 27, and having a single root and single canal (Figure 1) was suspected.

Figure 1: Preoperative IOPA.

Figure 2: Working length IOPA.

Figure 3: Post obturation IOPA.

Figure 4: Final restoration IOPA.

The tooth was anesthetized with 1.8mL (30 mg) 2% lignocaine containing 1 : 200,000 epinephrines followed by rubber dam isolation. Access opening with the aid of magnifying loupes (zumax 3.5X) of tooth 27 revealed a large single orifice and one single wide root buccolingually extending toward the root apex. Working length (WL) was determined with an apex locator (CanalPro Apex Locator, Coltene) and was confirmed with k-file (Figure 2). WL IOPA also confirmed the single-rooted maxillary second molar with a single canal. Root canal shaping was done with k-files using the conventional method of canal preparation and was irrigated with sodium hypochlorite. EDTA was used to remove the inorganic component of the root canal system, and a smear layer formed with filing the dentin. Saline was used as intermittent irrigation. Due to the wide nature of the canal, more attention was paid on chemical disinfection.

After canal preparation was done, IOPA was taken to confirm the fit of the master gutta percha cone. A lateral condensation technique of obturation with Apexit Plus as a sealer was used. Post obturation, IOPA was taken to examine filling of the root canal system (Figure 3). Follow-up IOPA two weeks after (Figure 4) was taken, and final restoration with amalgam was done, and the patient was advised for further treatment for Prosthesis.

Source: Mittal N et al. Case Rep Dent. 2020;2020:2829304.

High-speed cine-magnetic resonance imaging based on T2-weighted sequences for evaluation of velopharyngeal function

Velopharyngeal insufficiency can cause problems such as aspiration dysphonia, obstruction of drinking water, and stridor. In patients with cleft palate and those who have undergone surgeries for oral cancers, these dysfunctions lead to decreased quality of life (QoL). Real-time 3-T magnetic resonance imaging (MRI) that allows detailed evaluation of velopharyngeal function with appropriate temporal resolution has recently been developed5. However, 3-T MRI systems are not available in the majority of hospitals, and MRI techniques cannot be clinically applied for detailed evaluation of velopharyngeal function in most hospitals. New techniques using 1.5-T MRI systems need to be developed to provide precise and objective evaluation of velopharyngeal function.

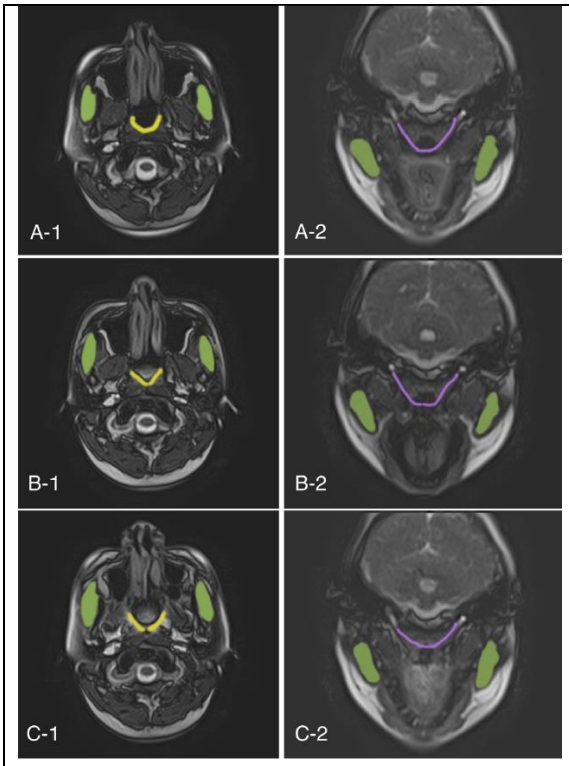

Measurement diagrams superimposed on the magnetic reaonance images of signal intensity in the quantitative analysis. Signal intensities are calculated on the cine-MRI during rest (A), phonation (B), and swallowing (C).

The objective was to introduce a new technique for visualizing the three dimensional (3D) movements of velopharyngeal-related muscles using high-speed cine-magnetic resonance imaging (MRI) based on T2-weighted sequences. The evaluation of phonation- and water swallowing-related events was performed in 11 healthy subjects. Specifically, whether cine-MRI could precisely visualize normal velopharyngeal function during these two events was examined. The 3D movements of the soft palate, superior pharyngeal constrictor muscles, and levator veli palatini muscles were visualized in all 11 subjects. A noteworthy finding was that the magnetic resonance signals of the superior constrictor pharyngeal muscles and the levator veli palatini muscles were significantly higher during phonation and during water swallowing than at rest. This initial study suggests that the 3D movements of velopharyngeal-related muscles can be successfully and precisely visualized without side effects. The magnetic resonance signal changes seen in the superior pharyngeal constrictor and levator veli palatini muscles using the technique described here should be useful to develop better methods of evaluation of velopharyngeal function.

Joujima T et al. Int J Oral Maxillofac Surg 2020 April. 49(4):e1-e10

Comparison of intraoral scan and desktop scan of study models

The last few decades have seen an increased use of digital technology in the field of dentistry. The most important ones being digital photographs, digital radiographs and digital models, which are becoming the norms in dental records. Digital study models were introduced to the field of orthodontics in the late 1990s and is now being gradually adopted in routine practice.

This was a prospective clinical study compared the measured values obtained from the plaster model, digital models created by scanning the plaster models and direct intraoral scanning with the values obtained from direct intraoral measurements.

A computer-aided design and manufacturing (CAD-CAM) system is an advanced technology that is being adopted in the field of orthodontics for diagnosis, treatment planning and documentation of patient records. Mesiodistal tooth width measurements of first premolars, canines, lateral incisors and central incisors, and transverse width measurement from mesial pit of right first premolar to mesial pit of left first premolar in both maxilla and mandible were obtained from direct intraoral measurement (gold standard), study model obtained from alginate impression, intraoral scanned image, and desktop scanned image of the study model.

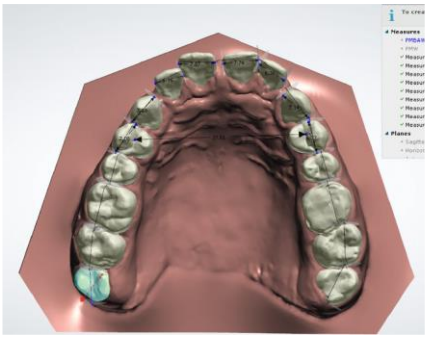

A P value > 0.05 was obtained in ANOVA indicating that there is no statistically significant difference in the measurements obtained by either of the methods. Conventional stone models and digital models obtained from intraoral scan and desktop scanning of plaster models are clinically reliable as the variations in measurements obtained from these methods were clinically negligible.

	Gold standard (direct intraoral)		Stone model		Intraoral scan		Desktop scan of stone model		
Tooth number	Mean (mm)	SD (mm)	Mean (mm)	SD (mm)	Mean (mm)	SD (mm)	Mean (mm)	SD (mm)	Significance
11	9.11	0.53	8.94	0.35	9.15	0.53	8.9	0.36	.55
12	7.68	0.52	7.39	0.42	7.59	0.36	7.37	0.62	.44
13	8.41	0.55	8.24	0.54	8.43	0.54	8.06	0.55	.41
14	7.60	0.36	7.50	0.52	7.52	0.47	7.46	0.48	.92
21	8.88	0.43	8.88	0.38	8.76	0.37	8.68	0.32	.60
22	7.45	0.41	7.48	0.48	7.34	0.46	7.35	0.44	.85
23	7.91	0.42	7.79	0.34	7.84	0.37	7.72	0.33	.72
24	7.53	0.46	7.47	0.52	7.58	0.38	7.47	0.50	.94
31	5.53	0.46	5.43	0.48	5.45	0.45	5.23	0.45	.55
32	6.11	0.26	6.09	0.28	6.04	0.33	5.87	0.32	.30
33	7.07	0.57	7.22	0.41	7.15	0.47	6.97	0.56	.73
34	7.71	0.57	7.72	0.51	7.62	0.54	7.50	0.61	.80
41	5.47	0.35	5.47	0.30	5.38	0.26	5.38	0.25	.81
42	6.10	0.28	6.07	0.37	6.13	0.29	6.00	0.30	.82
43	7.27	0.44	7.19	0.39	7.23	0.42	7.20	0.44	.96
44	7.40	0.63	7.42	0.51	7.33	0.58	7.31	0.56	.96
Interpremolar width in maxilla	34.62	2.86	34.60	2.82	34.74	2.67	34.55	2.79	.99
Interpremolar width in mandible	28.38	2.34	28.31	2.30	28.23	2.46	28.18	2.35	.99

Source: Murugesan A, J Orthod. 2020;14653125 20910755. doi:10.1177/1465312520910755